Artificial intelligence–assisted diagnosis of prostate cancer based on prostate biopsy

AUTHORS:
Dilber U. Ozsahin[1,2,3]
Declan I. Emegano[3]
Mubarak T. Mustapha[3]
Berna Uzun[3,4,*]
Ilker Ozsahin[3,5,*]

AFFILIATIONS:
[1]Department of Medical Diagnostic Imaging, College of Health Science, University of Sharjah, Sharjah, United Arab Emirates
[2]Research Institute for Medical and Health Sciences, University of Sharjah, Sharjah, United Arab Emirates
[3]Operational Research Center in Healthcare, Near East University, Mersin, Turkey
[4]Department of Mathematics, Near East University, Mersin, Turkey
[5]Brain Health Imaging Institute, Department of Radiology, Weill Cornell Medicine, New York, New York, USA
*Current: Department of Mathematical Sciences, Saveetha School of Engineering, Saveetha Institute of Medical and Technical Sciences (SIMATS), Chennai, India

CORRESPONDENCE TO:
Dilber Ozsahin

EMAIL:
dozsahin@sharjah.ac.ae

DATES:
Received: 02 May 2024
Revised: 08 Apr. 2025
Revised: 02 Oct. 2025
Accepted: 24 Oct. 2025
Published: 29 Jan. 2026

HOW TO CITE:
Ozsahin DU, Emegano DI, Mustapha MT, Uzun B, Ozsahin I. Artificial intelligence–assisted diagnosis of prostate cancer based on prostate biopsy. S Afr J Sci. 2026;122(1/2), Art. #18193. https://doi.org/10.17159/sajs.2026/18193

ARTICLE INCLUDES:
☒ Peer review
☐ Supplementary material

DATA AVAILABILITY:
☐ Open data set
☐ All data included
☒ On request from author(s)
☐ Not available
☐ Not applicable

EDITORS:
Pascal Bessong
Shane Redelinghuys

KEYWORDS:
AI, benign, malignant, biopsy, prostate cancer

FUNDING:
None

Prostate cancer is the most common solid tumour in men and the fifth leading cause of cancer death globally. It requires timely and accurate diagnostic procedures for the treatment processes. However, these procedures are labour intensive because of the histological examination of prostate biopsy specimens, which can be subject to interpretative variability. The present study was designed to evaluate the effectiveness of deep-learning algorithms specifically for the task of classifying prostate biopsy images into two categories: benign or malignant. The data set included 247 cancerous and 514 benign histological biopsy images. The data set was derived from patients aged between 39 and 80 years and who underwent prostate biopsies at the Federal Teaching Hospital in Lokoja, Nigeria, between 2019 and 2023. We augmented the data set to 10 000 histological images, after which 50 images from the same cohort were reserved for validation. Multiple Source Hierarchical Aggregation Neural Network, densely connected convolutional network, EfficientNet, Inception v3, MobileNet, ResNet-50, Visual Graphics Group 16 and Visual Graphics Group 19 were among the deep-learning models that were trained and verified. The results showed that densely connected convolutional network had an accuracy value of 0.96, with precision, recall and *F*1 scores of 1.00, 0.92 and 0.96, respectively, for benign cases and 0.93, 1.00 and 0.96, respectively, for malignant cases. Deep-learning models, especially the densely connected convolutional network, have shown great potential to distinguish between benign and malignant prostate images; as a result, they can significantly enhance prostate cancer diagnosis by improving diagnostic uniformity and efficacy for pathologists.

Significance:

- This study demonstrates the effectiveness of deep-learning models in enhancing artificial intelligence–assisted histopathological diagnosis by classifying prostate biopsy images.
- Artificial intelligence tools enhance accuracy and reliability, making them valuable resources for decision-makers.
- Additional validation in a variety of healthcare environments is needed to verify the real-world relevance as well as the generalising potential of our results.

Introduction

Prostate cancer is the most common type of cancer in men and a major global public health issue, accounting for 7.3%[1] of all male cancer diagnoses worldwide. Historically, prostate cancer diagnosis heavily relied on prostate-specific antigen tests, digital rectal examinations and various types of imaging techniques.[2] Although the aforementioned methods have made a substantial contribution to early prostate cancer detection, they are frequently constrained by both sensitivity and specificity, which can result in either overdiagnosis or misdiagnosis. The early diagnosis of prostate cancer is essential because it enhances diagnostic precision and therapeutic outcomes. The current standard for diagnosing prostate cancer is biopsy, especially transrectal ultrasonography guided biopsy, which is commonly used.[3] However, transrectal ultrasonography is constrained by sampling errors because of the different features of prostate tumours, variability among pathologist assessments and, above all, it is highly invasive. Because of the limitations highlighted, there is a need for enhanced evaluation techniques that can improve accuracy and minimise invasiveness.

The complexity of human interpretation and the challenges faced by pathologists due to their large caseload underscore the need for artificial intelligence (AI) solutions in diagnosis.

Recently, AI has been a revolutionary force in numerous healthcare sectors, revolutionising diagnosis, treatment and the management of patient data.[4] It is currently being used in health care to speed up diagnostic procedures by providing up-to-date recommendations. AI-driven image analysis can evaluate medical images and identify small changes as early signs of diseases. In histopathology, AI could be used to assess histological slides and classify malignant tumours with high precision.[5] AI-driven image analysis has advanced modern medicine by recognising prostate cancers and inflammatory markers, especially in radiographic imaging. Early disease diagnosis is crucial for preventing severe health complications for patients. AI algorithms can evaluate data sets on medical images and look for tiny alterations that could be early signs of diseases. In a histopathological context, AI algorithms play a useful role in assessing histological slides in the field of pathology. AI, most notably through machine- and deep-learning models, has exhibited exceptional abilities in analysing multifaceted medical data, such as images, tissue pathology and other biological data.[6] The AI models identify intricate structures and latent attributes that are not visible to human observation, resulting in an increasingly accurate diagnosis. As a result, AI's ability to identify tumour sites and structural variants and its strong image interpretation have made it a significant health speciality.[7] Furthermore, advancements in AI, particularly machine- and deep-learning techniques, are transforming the diagnosis of prostate cancer, improving patient outcomes and reducing mortality rates, enabling efficient and precise pathologic evaluations. AI's strong interaction with medical images has led to a boom in various health specialities in the 21st century, providing potential insights into cancer diagnosis and pathological contexts.[8] However, successful implementation requires challenges such as data quality, interoperability and regulatory permission to be addressed. The quantity and quality of data are crucial, and compatibility between electronic health records, image archives and healthcare communication systems is also essential.[9]

Literature review

Several lines of evidence have demonstrated considerable potential for AI in diagnosing prostate cancer using prostate biopsy. For instance, Ström et al.[10], using a population-based approach, demonstrated the efficacy of AI in the diagnosis and grading of prostate cancer from prostate biopsies. In the same vein, Perincheri et al.[11] employed a high level of accuracy for the detection of prostate cancer and found that it had a high level of diagnostic accuracy, showcasing the dependability of AI and its successful implementation in the diagnosis. Furthermore, da Silva et al.[12] focused on the performance of prostate auto-detection systems using AI in practical scenarios. Their findings suggest that the AI auto-detection system can distinguish between patients who can undergo complete histopathological assessment and those who cannot. The literature review by Bhattacharya et al.[13] indicates that AI models are employed for the detection of prostate cancer, showing the importance of these AI models in radiology and histology for the detection of cancers from images. Ultimately, the aforementioned scholars have demonstrated the significant effect of AI on diagnosing prostate cancer using biopsy samples. This has the potential to improve both the precision and the effectiveness of prostate cancer diagnosis. On top of that, the incorporation of deep-learning computational techniques into AI systems has also demonstrated notable potential in improving the readability of biopsy images, thereby assisting oncologists in making precise diagnoses.[14] In a recent study, Zhu et al.[15] proposed an explanatory result on the management of prostate cancer. The study suggested that AI-based methodologies could assist pathologists in reducing their workload and developing treatment recommendations for prostate cancer while also providing an overview of the procedure and challenges encountered. In this study, our goal was to evaluate and enhance the potential of numerous AI deep-learning models for the classification of prostate biopsy samples as either benign or malignant. The results of this study enhance the diagnostic accuracy as well as the efficiency of the prostate cancer diagnostic workflow.

Materials and methods

Data set description

The data set in our study originated from the Federal Teaching Hospital in Lokoja, Nigeria, collected from men aged 39–80 years who, because of elevated prostate-specific antigen, were recommended for biopsy by the physician. The data set was collected between January 2019 and December 2023. The physician performed a transrectal ultrasound-guided biopsy because it is the most common successful biopsy method. The prostate biopsy tissues were then preserved in 10% buffered formalin to avoid autolysis and putrefaction and, above all, to maintain the morphological characteristics of the tissue. The tissue (Figure 1a) was cut using a surgical blade and placed in a cassette for grossing. The tissue was dehydrated using grades of alcohol (80%, 90% and 100%) solution, then cleared using xylene so that the paraffin wax could infiltrate the tissue (Figure 1b) well at temperatures between 40 °C and 70 °C before processing (Figure 1c). Next the tissue underwent embedding, in which the paraffin block (cool paraffin wax and tissue) was stored at room temperature before sectioning (Figure 1d). The tissue was sectioned using a microtome and then cut into 3–5 μm sections before staining. We used haematoxylin and eosin (Figure 1e), a conventional technique for examining disease and human anatomy[16], to stain the tissue. Due to its strong affinity for the acidic components of the tissue, haematoxylin[17] stains cell nuclei in shades of purple[18], whereas eosin produces pink colouration on the cytoplasmic components of the tissue, allowing for their microscopic visibility. The tissue sections were then viewed under the microscope (Figure 1f and 1g) using a 10× objective and 100× magnification. The image in Figure 2 forms the basis of our data set for this study. As a result, we had 748 (214 for malignant and 514 for benign) histological images comprising the data set for this study.

Image and data processing

The images (Figure 2), saved as a joint photographic experts group (JPEG), were then repurposed into uniform portable network graphics (PNG) files

Figure 1: Prostate tissue sectioning and processing. (a) Tissue grossing; (b) fixation of tissue in formalin; (c) automated tissue processing; (d) paraffin wax embedding; (e) haematoxylin and eosin staining; (f) stained tissue slide; (g) microscopic examination.

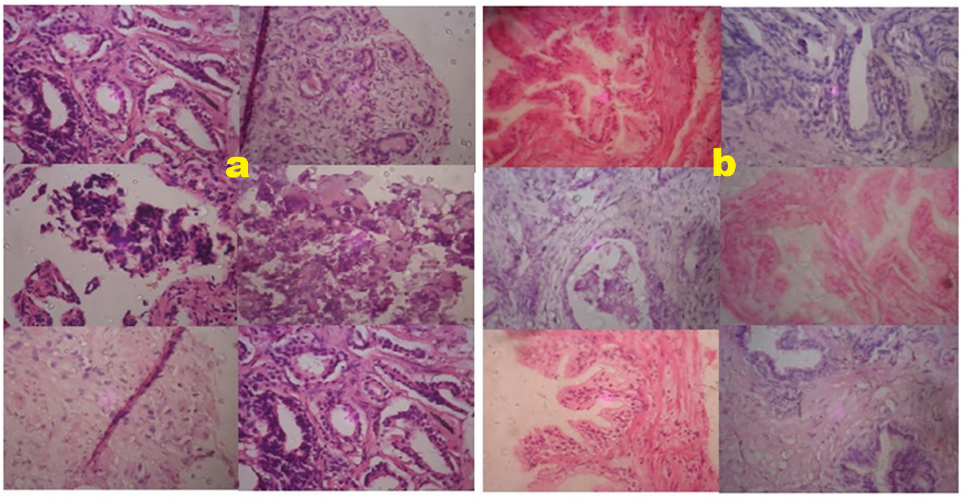

Figure 2: (a) Malignant histological prostate slides. (b) Benign histological prostate slides.

Table 1: Distribution of the augmented prostate tissue histological images data set by prostate-specific antigen (PSA) type

PSA type	Original size	Initialise size	Image mode	Output	Processing time (s)	Reserved data for validation
Benign	514	464	4320 × 3240	10 000	9.025	50
Malignant	247	197	4320 × 3240	10 000	14.025	50

to maintain data quality and support various colour depths, including index, greyscale and true colours, with the combination of alpha transparency. Then, Python 9.2.0 and Scikit-image version 0.19.3 were used to augment the data set, as recorded in Table 1. Augmentation improves model generalisation, enhances robustness and reduces overfitting.

Also, augmentation reduces the cost of labelling and the collection of data. Above all, the accuracy of the model will be increased. The output of the augmentation was 10 000 images, which were used in this study. The augmented data set was then subjected to image denoising (noise reduction).

Denoising

Image denoising is a process that improves the quality of digital images by cleaning up muddled digital content. Noise, caused by factors such as sensor limits, interference or the environment, can significantly reduce the sharpness and detail of an image. We also employed spatial denoising, which determines each pixel's greyscale value and domain and also uses mathematical analysis to transform the features of image data and background noise. In addition, a deep convolutional neural network autoencoder was used, which can learn useful data characteristics and representations to recreate the original image without human supervision.[19] The autoencoder consists of a deep neural network encoder and decoder, with the encoder processing images before sending them to the decoder, which analyses hidden coding and generates a new version of the original image.

Proposed models

In this study, we used the deep-learning models Multiple Source Hierarchical Aggregation Neural Network (MSHA), densely connected convolutional network (DenseNet), EfficientNet, Visual Graphics Groups (VGG19 and VGG16), Inception v3, ResNet-50 and MobileNet. MSHA is flexible and combines image categorisation and object identification in a single architecture, thereby eliminating the need for multiple models.[20] MSHA features batch normalisation, dropout layers, residual connections and focused attention techniques. DenseNet addresses vanishing gradients and feature reuse in deep-learning networks. DenseNet differs from traditional convolutional neural networks by providing a feed-forward connection to all layers, enabling direct supervision through compact pathways in backward propagation.[21] DenseNet's efficiency also enhances flow for optimisation and reduces overfitting, making it a valuable tool for deep learning.[21] EfficientNet improves classification accuracy by focusing on model depth and width resolution. EfficientNet also ensures that the network's overall dimensions are in equilibrium with available resources, resulting in better results.[22] Similarly, Inception v3 stands out for its speed and precision, making it popular in image categorisation due to its fewer parameters and more depth, thus removal of unfitting.[23] However, for MobileNet, a self-learning mechanism to automatically extract features with high accuracy, reducing model parameters and computation time is achieved. ResNet 50 has 50 layers of architecture, which improves the model's accuracy through a vanishing gradient.[24] VGG16 is a widely used deep-learning model for image categorisation. The VGG16 model has been updated to enhance its depth for more sophisticated characteristics. The 19-layer architecture, derived from the VGG16 model, incorporates three fully connected layers and a rectified linear unit activation function, enabling it to detect and learn from intricate patterns in input data.[25]

Table 2: Evaluation metrics

Model	Calculation formula
Accuracy	$\frac{TP + TN}{TP + TN + FP + FN}$
Precision	$\frac{TP}{TP + FN}$
Recall	$\frac{TP}{TP + TN}$
$F1$ score	$2 \times \frac{Precision \times Recall}{Precision + Recall}$

TP, True positive; TN, true negative; FP, false positive; FN, false negative

Evaluation metrics

The effectiveness of the models was evaluated across several domains using model evaluation metrics. The evaluation metrics are accuracy, precision, recall and $F1$ score. Accuracy measures the model's performance by dividing the sum of true positives and true negatives by the overall number of instances. Precision indicates how accurately the model makes predictions, while recall focuses on accurately identifying pertinent instances. Similarly, the $F1$ score is a harmonic mean that balances precision and recall. The overall evaluation metric is presented in Table 2.

Training and validation of models

Our initial data set contained 514 images for benign and 247 images for cancerous tissue. We then removed 50 images from benign and 50 from cancerous to be used as a validation data set. The remaining 464 benign and 197 cancerous prostate images were then augmented to 10 000 images for benign and 10 000 for cancerous, as recorded in Table 1. The augmentation ensures data enhancement, robustness and variability. We then randomly split the augmented images into training (70%) and testing (30%). The reserved data set is only used for validation, and it ensures model generalisability and robustness. The data set was simulated in Python and then processed uniformly (training, testing and validation) in batches of 32. This strategy enhances the model's learning process, thus ensuring that the error computations are accurate and guaranteeing that the model is progressing in the correct direction. We shuffled the training and validation data sets to avoid memorising the effect of a particular trend and ensure every training phase incorporated a diverse range of data sets. Finally, we used 50 epochs to train the model and added a callback and early stopping for regularisation while maintaining validity loss. This is not a standard rule and is dependent on the individual researcher's discretion.

Methodological overview

Figure 3 depicts the sequential process of data collection, preprocessing, modelling, training, validation and findings, presenting an easily understood graphic illustration of the research's design.

Results

The overall result of AI-assisted diagnosis of prostate cancer based on prostate biopsy using deep-learning models is recorded in Table 3. The values in Table 3 indicate that DenseNet had an accuracy value of 0.98 with precision, recall and $F1$ scores of 1.00, 0.92 and 0.96, respectively, for benign cases and 0.93, 1.00 and 0.96, respectively, for malignant cases. ResNet 50 and VGG16 ranked low because of the difficulty in identifying benign cases.

We thoroughly evaluated how well the model worked by providing model training and testing losses (Table 4), with area under the curve (AUC) receiver operating characteristic (ROC) values. Again, AUC measures the discriminating capability of the deep-learning models. Models with higher AUCs performed better.

Moreover, the learning curve and confusion matrix for each deep-learning model are also presented. The learning curve shows the dynamics spanning each of the training epochs by graphing the accuracy (Figure 4) and loss curves (Figure 5) for training as well as validation data sets. This helped us identify problems such as underfitting or overfitting through comparative analysis of both losses.

The confusion matrix (Figure 6) also shows the detailed performance of the models as true positive, true negative, false positive and false negative results. Furthermore, the model's performance was also evaluated using the ROC curve, providing a graphical representation of each of the deep-learning models used in this study. Graphically, the ROC shows the true positive rate (sensitivity) and false positive rate (1-specificity) of our study as shown in Figure 7.

Discussion

We analysed the performance of different deep-learning architectures for prostate cancer classification using histological images. DenseNet demonstrated impressive adaptability in image classification and object recognition evaluations, outperforming existing architectures such as

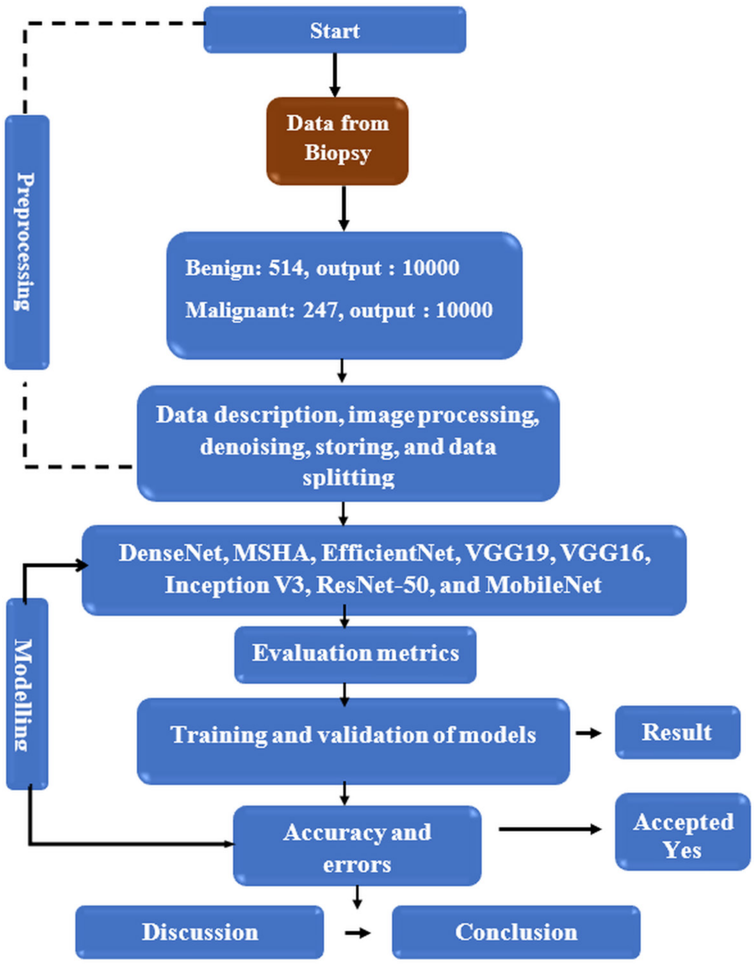

Figure 3: Study flow chart.

Table 3: Performance evaluation metrics

Model		Accuracy	Precision	Recall	*F*1 score
	Benign		1.0	0.92	0.96
DenseNet		0.98			
	Malignant		0.93	1.0	0.96
	Benign		1.00	0.86	0.92
MSHA		0.93			
	Malignant		0.88	1.00	0.93
	Benign		1.00	0.92	0.96
EfficientNet		0.96			
	Malignant		0.93	1.00	0.96
	Benign		0.98	0.92	0.95
Inception v3		0.95			
	Malignant		0.92	0.98	0.95
	Benign		0.98	0.94	0.96
MobileNet		0.96			
	Malignant		0.94	0.98	0.96
	Benign		0.86	0.38	0.53
ResNet 50		0.66			
	Malignant		0.60	0.94	0.73
	Benign		1.00	0.82	0.90
VGG19		0.91			
	Malignant		0.85	1.00	0.92
	Benign		0.86	0.38	0.53
VGG16		0.66			
	Malignant		0.60	0.94	0.73

MSHA, EfficientNet, Inception v3 and ResNet-50. This highlights the importance of considering efficiency and complexity in model-specific task selection. VGG19, VGG16 and MobileNet also demonstrated fine-tuning characteristics for optimal performance in identifying and categorising benign and malignant prostate cases. DenseNet's successful integration of image categorisation and object recognition in a single architecture represents a paradigm shift in deep-learning applications.

Clinically, the results of this study have significant implications for the diagnosis of prostate cancer. For instance, the accuracy and *F*1 scores of DenseNet illustrate the capacity to augment and improve conventional histopathological assessments. The results, when integrated into clinical workflow, will help oncologists to ensure diagnostic precision and consistency. In addition, it could help in the early detection of cancer, which greatly influences treatment success.

As recorded in Table 3, DenseNet models performed exceptionally well in the test, displaying a high degree of efficiency and accuracy. Comparing our findings with those of other published articles, we found that our study, in terms of the number of images in the data set, outnumbered Campanella et al.[26] However, with 12 132 images as a data set, the Multiple Instance Learning-Recurrent Neural Network model used by Campanella et al. produced a higher AUC value (0.99) compared with this study (0.96). This mismatch may result from their more extensive initial study data, which obviously covered broader histological heterogeneity. Our study's data set

Table 4: Model testing losses and area under the curve (AUC) receiver operating characteristic (ROC) values

Model	Test loss	AUC ROC
DenseNet	0.13	0.9988
MSHA	0.31	0.9941
EfficientNet	0.17	0.9752
Inception v3	0.17	0.9764
MobileNet	0.26	0.9632
VGG16	0.59	0.8892
ResNet 50	0.59	0.8696
VGG19	0.32	0.9560

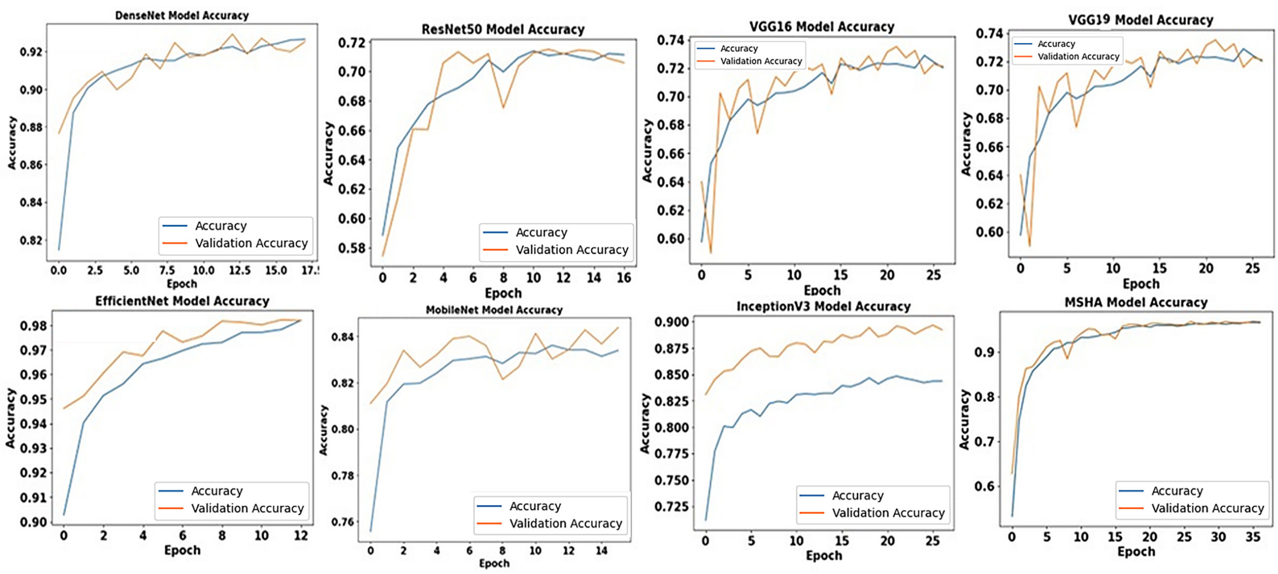

Figure 4: Accuracy curve of the DenseNet and other models.

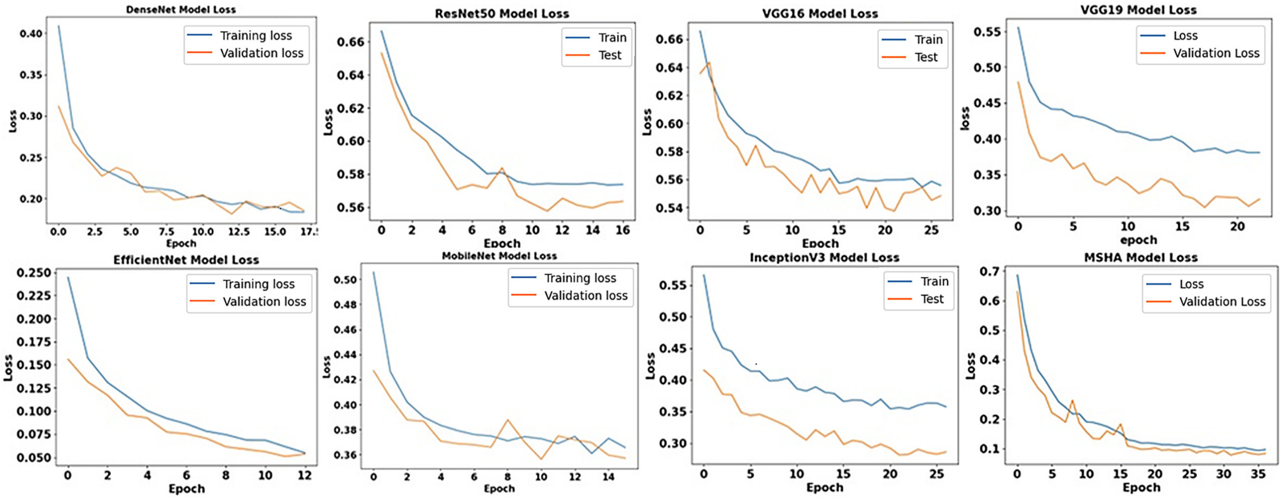

Figure 5: Loss curve of the DenseNet and other models.

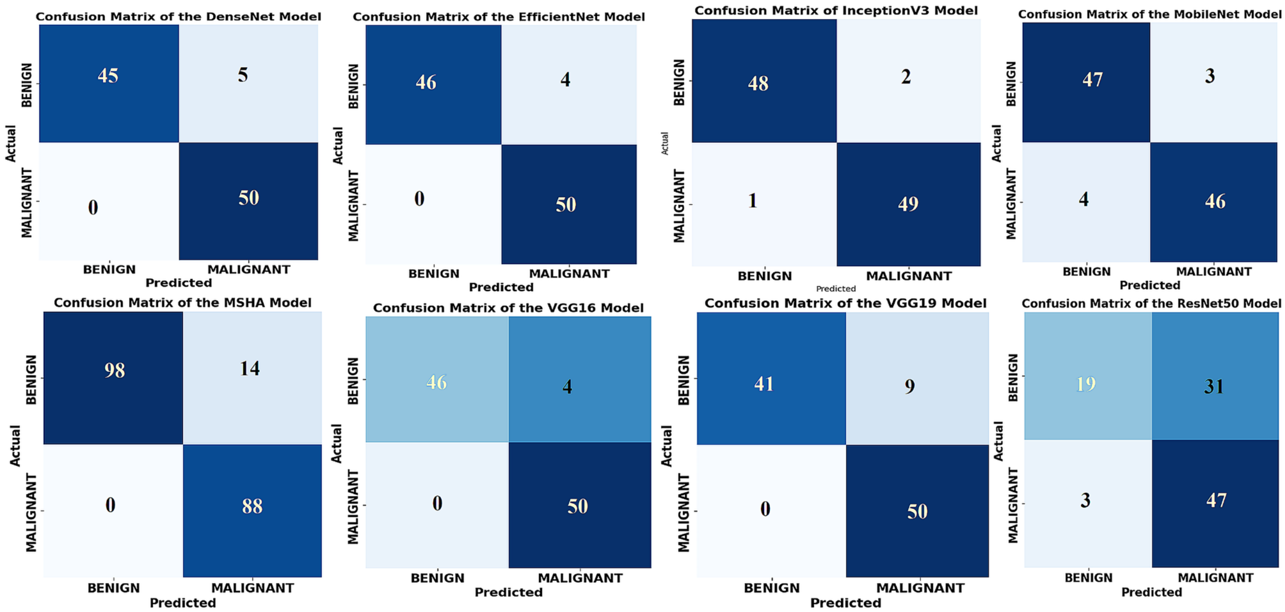

Figure 6: Confusion matrix of the deep-learning models used in this study.

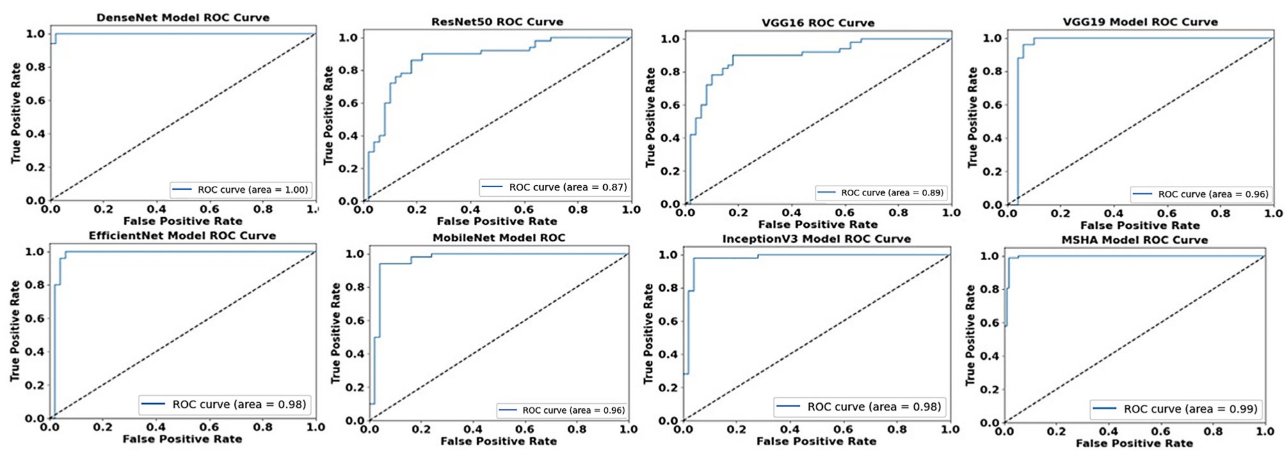

Figure 7: Receiver operating characteristic (ROC) curve of the deep-learning models used in this study.

was augmented to 20 000 images from 761 slides, which may restrict feature variety. Next, our study showed superior performance compared with Vazzano et al.[27] Convolutional neural network results, with 30 patients as a data set, were 0.97 for specificity, 0.99 for sensitivity and 0.76 for the correlation coefficient. Similarly, our study showed superior performance as compared with Ordones et al.[28] Ordones et al.'s original data before augmentation were 428 histological images from a biopsy, compared with our original 728 histological samples from biopsy. Ordones et al.'s study recorded 0.8 and 0.73 as ROC and accuracy values, compared with 0.87 and 0.65 for our study. However, after modification, the deep-learning architecture was used by Ordones et al. to improve prostate cancer diagnosis. The ResNet50 model values outperformed this study in terms of *F*1 scores of 95.2%. This discrepancy could originate from the use of tailored preprocessing, warranting investigation in additional study sections (iteration). Swiderska-Chadaj et al.[29] used 582 prostate whole slide images; DenseNet and EfficientNet were the best-performing models, with 0.92 and 0.83 as AUC ROC values, as compared with 0.99 and 0.98, respectively, in our study. Finally, Gour et al.[30] used ResNet50, VGG16 and 19, Inception v3 and EfficientNet, but our study outperformed their best model, EfficientNet, with an accuracy value of 96% compared with Gour et al.'s 90%.

Limitations

The data set used in this study was from a single healthcare centre, which may cause bias given that prostate cancer features differ among populations. In our subsequent research, we hope to integrate multicentre data and augment the number of original slides to improve robustness, hence resolving the limitation regarding data set size. Although 761 slides (from various patients) were adequate for this proof of concept, an expansion to thousands of slides could further substantiate the models.

Conclusion

This study shows that AI-assisted diagnosis using deep-learning models markedly improves the accuracy and efficiency of classifying biopsy images. We utilised the deep-learning architectures DenseNet, MSHA, EfficientNet, Inception v3, MobileNet, ResNet 50, VGG16 and VGG19 to categorise histological prostate tissue images. DenseNet had an accuracy value of 0.96 with precision, recall and *F*1 scores of 1.00, 0.92 and 0.96, respectively, for benign cases and 0.93, 1.00 and 0.96, respectively, for malignant cases. The results of this study are highly significant as they highlight the capability of AI to support pathologists' clinical evaluation of prostate cancer patients, guaranteeing more accurate and consistent diagnoses of prostate cancer.

Acknowledgements

We are grateful to the entire staff of the Histopathology Department for their moral support and active participation during the sectioning which contributed to the success of this study.

Data availability

The data supporting the results of this study are available upon request to the corresponding author.

Declarations

We have no competing interests to declare. We have no AI or LLM use to declare. The Health Research Ethics Committee of the Federal Teaching Hospital in Lokoja, Nigeria, approved this study (FMCL/HREC/Vol.1/2023/192).

Authors' contributions

D.U.O.: Project leadership, project administration. D.I.E.: Data curation, conceptualisation, investigation, writing – original draft. M.T.M.: Formal analysis. B.U.: Methodology, formal analysis. I.O.: Validation, writing – review and editing. All authors read and approved the final manuscript.

References

1. Wang L, Lu B, He M, Wang Y, Wang Z, Du L. Prostate cancer incidence and mortality: Global status and temporal trends in 89 countries from 2000 to 2019. Front Public Health. 2022;10, Art. #811044. https://doi.org/10.3389/fpubh.2022.811044
2. Klein C, Bosc N, Marty S, Calen L, Debard C, Robert G, et al. Prostate cancer patients' perceptions regarding the relevance of a digital rectal examination during their follow-up after radiation therapy. Cancer Med. 2025;14(1), e70563. https://doi.org/10.1002/cam4.70563
3. Wang X, Xie Y, Zheng X, Liu B, Chen H, Li J, et al. A prospective multi-center randomized comparative trial evaluating outcomes of transrectal ultrasound (TRUS)-guided 12-core systematic biopsy, mpMRI-targeted 12-core biopsy, and artificial intelligence ultrasound of prostate (AIUSP) 6-core targeted biopsy for prostate cancer diagnosis. World J Urol. 2023;41(3):653–662. https://doi.org/10.1007/s00345-022-04086-0
4. Garg PP, Jayashree J, Vijayashree J. Revolutionizing healthcare: The transformative role of artificial intelligence. In: Singh A, Singh KK, Izonin I, editors. Responsible and explainable artificial intelligence in healthcare. London: Academic Press; 2025. p. 1–23. https://doi.org/10.1016/B978-0-443-24788-0.00001-7
5. Elemento O, Leslie C, Lundin J, Tourassi G. Artificial intelligence in cancer research, diagnosis and therapy. Nat Rev Cancer. 2021;21(12):747–752. https://doi.org/10.1038/s41568-021-00399-1
6. Li M, Jiang Y, Zhang Y, Zhu H. Medical image analysis using deep learning algorithms. Front Public Health. 2023;11, Art. #1273253. https://doi.org/10.3389/fpubh.2023.1273253
7. Fu Y, Jung AW, Torne RV, Gonzalez S, Vöhringer H, Shmatko A, et al. Pan-cancer computational histopathology reveals mutations, tumor composition, and prognosis. Nat Cancer. 2020;1(8):800–810. https://doi.org/10.1038/s43018-020-0085-8
8. Sun F, Zhang L, Tong Z. Application progress of artificial intelligence in tumor diagnosis and treatment. Front Artif Intell. 2025;7, Art. #1487207. https://doi.org/10.3389/frai.2024.1487207
9. Bouschery SG. Artificial intelligence in health care: Trust, privacy, and the acceptance of AI doctors. Acad Manag Proc. 2021;2021(1), Art. #15900. https://doi.org/10.5465/AMBPP.2021.15900abstract
10. Ström P, Kartasalo K, Olsson H, Solorzano L, Delahunt B, Berney DM, et al. Artificial intelligence for diagnosis and grading of prostate cancer in biopsies: A population-based, diagnostic study. Lancet Oncol. 2020;21(2):222–232. https://doi.org/10.1016/S1470-2045(19)30738-7
11. Perincheri S, Levi AW, Celli R, Gershkovich P, Rimm D, Morrow JS, et al. An independent assessment of an artificial intelligence system for prostate cancer detection shows strong diagnostic accuracy. Mod Pathol. 2021;34(8):1588–1595. https://doi.org/10.1038/s41379-021-00794-x
12. da Silva LM, Pereira EM, Salles PG, Godrich R, Ceballos R, Kunz JD, et al. Independent real-world application of a clinical-grade automated prostate cancer detection system. J Pathol. 2021;254(2):147–158. https://doi.org/10.1002/path.5662
13. Bhattacharya I, Khandwala YS, Vesal S, Shao W, Yang Q, Soerensen SJC, et al. A review of artificial intelligence in prostate cancer detection on imaging. Ther Adv Urol. 2022;14, Art. #17562872221128791. https://doi.org/10.1177/17562872221128791
14. Singh A, Wan M, Harrison L, Breggia A, Christman R, Winslow RL, et al. Visualizing decisions and analytics of artificial intelligence-based cancer diagnosis and grading of specimen digitized biopsy: Case study for prostate cancer. In: Companion Proceedings of the 28th International Conference on Intelligent User Interfaces; 2023 March 27–31; Sydney, Australia. New York: Association for Computing Machinery; 2023. p. 166–170. https://doi.org/10.1145/3581754.3584177
15. Zhu L, Pan J, Mou W, Deng L, Zhu Y, Wang Y, et al. Harnessing artificial intelligence for prostate cancer management. Cell Rep Med. 2024;5(4), Art. #101506. https://doi.org/10.1016/j.xcrm.2024.101506
16. Rana A, Lowe A, Lithgow M, Horback K, Janovitz T, Da Silva A, et al. Use of deep learning to develop and analyze computational hematoxylin and eosin staining of prostate core biopsy images for tumor diagnosis. JAMA Netw Open. 2020;3(5), e205111. https://doi.org/10.1001/jamanetworkopen.2020.5111
17. Ortiz-Hidalgo C, Pina-Oviedo S. Hematoxylin: Mesoamerica's gift to histopathology. Palo de Campeche (Logwood Tree), pirates' most desired treasure, and irreplaceable tissue stain. Int J Surg Pathol. 2019;27(1):4–14. https://doi.org/10.1177/1066896918787652
18. Lahiani A, Klaiman E, Grimm O. Enabling histopathological annotations on immunofluorescent images through virtualization of hematoxylin and eosin. J Pathol Inform. 2018;9(1), Art. #1. https://doi.org/10.4103/jpi.jpi_61_17

19. Ashour AS, Guo Y. Advanced optimization-based neutrosophic sets for medical image denoising. In: Guo Y, Ashour AS, editors. Neutrosophic set in medical image analysis. London: Academic Press; 2019:101–121. https://doi.org/10.1016/B978-0-12-818148-5.00005-9

20. Abdel-Basset M, Hawash H, Chakrabortty RK, Ryan M. PV-Net: An innovative deep learning approach for efficient forecasting of short-term photovoltaic energy production. J Clean Prod. 2021;303, Art. #127037. https://doi.org/10.1016/j.jclepro.2021.127037

21. Hemalatha J, Roseline SA, Geetha S, Kadry S, Damaševičius R. An efficient DenseNet-based deep learning model for malware detection. Entropy. 2021;23(3), Art. #344. https://doi.org/10.3390/e23030344

22. Antonio B, Moroni D, Martinelli M. Efficient adaptive ensembling for image classification. Expert Syst. 2025;42(1), e13424. https://doi.org/10.1111/exsy.13424

23. Dong N, Zhao L, Wu CH, Chang JF. Inception v3 based cervical cell classification combined with artificially extracted features. Appl Soft Comput. 2020;93, Art. #106311. https://doi.org/10.1016/j.asoc.2020.106311

24. Fulton LV, Dolezel D, Harrop J, Yan Y, Fulton CP. Classification of Alzheimer's disease with and without imagery using gradient boosted machines and ResNet-50. Brain Sci. 2019;9(9), Art. #212. https://doi.org/10.3390/brainsci9090212

25. Montaha S, Azam S, Rafid AKMRH, Ghosh P, Hasan MdZ, Jonkman M, et al. BreastNet18: A high accuracy fine-tuned VGG16 model evaluated using ablation study for diagnosing breast cancer from enhanced mammography images. Biology. 2021;10(12), Art. #1347. https://doi.org/10.3390/biology10121347

26. Campanella G, Hanna MG, Geneslaw L, Miraflor A, Werneck Krauss Silva V, Busam KJ, et al. Clinical-grade computational pathology using weakly supervised deep learning on whole slide images. Nat Med. 2019;25(8):1301–1309. https://doi.org/10.1038/s41591-019-0508-1

27. Vazzano J, Johansson D, Hu K, Eurén K, Elfwing S, Parwani A, et al. Evaluation of computer-aided detection software for prostate cancer prediction: Excellent diagnostic accuracy independent of preanalytical factors. Lab Invest. 2023;103(12), Art. #100257. https://doi.org/10.1016/j.labinv.2023.100257

28. Ordones FV, Vermeulen L, Hooshyari A, Scholtz D, Kawano P, de Andrade GM, et al. MP31-02 machine learning outperform traditional approaches in predicting clinically significant prostate cancer. J Urol. 2024;211(5S), e503. https://doi.org/10.1097/01.JU.0001008936.35187.0b.02

29. Swiderska-Chadaj Z, de Bel T, Blanchet L, Baidoshvili A, Vossen D, van der Laak J, et al. Impact of rescanning and normalization on convolutional neural network performance in multi-center, whole-slide classification of prostate cancer. Sci Rep. 2020;10(1), Art. #14398. https://doi.org/10.1038/s41598-020-71420-0

30. Gour M, Jain S, Shankar U. Application of deep learning techniques for prostate cancer grading using histopathological images. In: Raman B, Murala S, Chowdhury A, Dhall A, Goyal P, editors. Computer vision and image processing. Cham: Springer International Publishing; 2022. p. 83–94. https://doi.org/10.1007/978-3-031-11346-8_8